Journal of Photochemistry and Photobiology A: Chemistry 333 (2017) 49–55

Contents lists available at ScienceDirect

Journal of Photochemistry and Photobiology A: Chemistry

journal homepage: www.elsevier.com/locate/jphotochem

On the apparent visible-light and enhanced UV-light photocatalytic activity of nitrogen-doped TiO_2 thin films

Raul Quesada-Cabrera[a,*], Carlos Sotelo-Vázquez[a], Miguel Quesada-González[a], Elisenda Pulido Melián[b], Nicholas Chadwick[a], Ivan P. Parkin[a,*]

[a] University College London, Department of Chemistry, Christopher-Ingold Laboratories, 20 Gordon Street, London WC1H 0AJ, United Kingdom
[b] Universidad de Las Palmas de Gran Canaria, Grupo de Fotocatálisis y Electroquímica Aplicada al Medio-Ambiente (FEAM), Parque Científico-Tecnológico, Las Palmas de Gran Canaria 35017, Spain

ARTICLE INFO

Article history:
Received 20 May 2016
Received in revised form 9 September 2016
Accepted 7 October 2016
Available online 11 October 2016

Keywords:
Nitrogen-doped titania
Surface species
Extrinsic UV activity
Apparent visible light activity
Chemical vapor deposition
Photocatalysis

ABSTRACT

Nitrogen-doped titania (N—TiO_2) thin films were synthesized using atmospheric-pressure chemical vapor deposition (APCVD) using ammonia, *tert*-butylamine or benzylamine as the nitrogen source. The influence of these precursors on the structural, morphological and optical absorption properties of the films was studied using X-ray diffraction (XRD), Raman spectroscopy, Scanning electron microscopy (SEM) and UV/Vis spectroscopy. The chemical state and location of the nitrogen species in the films was investigated using X-ray photoelectron spectroscopy (XPS). The photocatalytic activity of films with similar structural properties was evaluated during degradation of stearic acid under UVA and visible light illumination. A previous study established a potential photosensitization mechanism involving surface N groups with binding energy of ~400 eV, which would result in extrinsic enhanced UV activity of the N—TiO_2 films. Here, an empirical approach was adopted in order to establish correlation between structural features, nitrogen content and photocatalytic properties of these films. Within the thickness range considered, the photocatalytic activities of the undoped TiO_2 films were consistent with their diffraction features (peak intensities and sharpness). Nevertheless, the activities of the N—TiO_2 films did not follow the same trend but it was consistent with their nitrogen content. Further evidence is provided on the participation of nitrogen species on the enhanced UV activity of N—TiO_2 films and the impact of surface N—O groups such as N—O—Ti—O (or O—N—Ti—O) and bulk substitutional nitrogen groups is discussed. Discussion is also provided on the apparent visible light activity of the N—TiO_2 films.

1. Introduction

Nitrogen-doped titania (N—TiO_2) materials have become archetypical of visible-light active photocatalysts [1–6], although the origin of their photocatalytic activity is still a matter of debate. This is largely due to the ambiguous assignment of N species based on X-ray photoelectron spectroscopy (XPS) studies [1,2,7]. Nevertheless, general consensus has assigned two main positions for nitrogen in the TiO_2 lattice, namely as substitutional (N^{3-}, replacing oxygen) and interstitial (N^0, N . . . O groups with lattice oxygen) species with binding energies of *ca.* 396 and 400 eV, respectively [8,9]. These groups will be henceforth referred to as N(s) and N(i), respectively, in this work. Unfortunately, a wide range of N-containing species such as NO^{x-}, NH_x, etc. are also expected at binding energies around 400 eV [8,10,11] and these may influence on optical absorption and photocatalytic activity of the films.

The incorporation of nitrogen in TiO_2 typically results in the red shift of the absorption onset and, often, additional features in the absorption spectrum of N—TiO_2 films. This has been widely explained on the basis of localized N *2p* midgap energy states above the upper O *2p* valence band in anatase TiO_2 [3,12]. It has been calculated that N(s) and N(i) species would introduce localized states respectively at 0.14 eV and 0.73 eV above the valence band of TiO_2 [10]. Unfortunately, the corresponding shift in optical absorption has not been unambiguously correlated with the N content in these materials.

Further complications arise when considering the potential role of oxygen vacancies in the visible light activity of N—TiO_2 materials [2]. The incorporation of N^{3-} groups in the TiO_2 lattice is expected to result in the formation of oxygen vacancies [10]. Some authors have associated the activity of N—TiO_2 materials

* Corresponding authors.
E-mail addresses: r.quesada@ucl.ac.uk (R. Quesada-Cabrera), i.p.parkin@ucl.ac.uk (I.P. Parkin).

http://dx.doi.org/10.1016/j.jphotochem.2016.10.013

with an optimum load of defect sites in the form of Ti≡N triple bonds [13]. It has also been shown that oxygen vacancies may induce optical absorption above 500 nm [14]. Nevertheless, recent electron paramagnetic resonance (EPR) studies have shown an increase in the rate of formation of photogenerated charges in N—TiO_2 upon the synergistic effect of visible (around 400 nm) and near-infrared light [15]. The authors proposed a mechanism involving intra band gap NO^{x-} states located just above the valence band of TiO_2. In this double excitation process, the visible light component would promote electrons from the NO^{x-} states into the conduction band whilst NIR frequencies would excite electrons from the valence band to the NO^{x-} centers. This mechanism thus requires the presence of N species with binding energies at 400 eV (N(i)).

It is interesting to note that visible light activity has also been observed in N – *modified*, rather than *doped*, TiO_2 materials. *Nosaka et al.* [16] reported the deactivation of N—TiO_2 materials during photo-induced oxidation of 2-propanol in the visible range. These authors attributed the decrease in activity as due to either the presence of surface sensitizing by-products or the release of nitrogen from the TiO_2 lattice, as confirmed by a concomitant decrease of surface N(s) groups (396.5 eV). In a previous work [17], we demonstrated the sensitization of N—TiO_2 films by N(i) species under UVA illumination. It was shown that the initially enhanced UV light activity dropped abruptly alongside an important weakening of the binding energy peak at 400 eV. The apparent enhanced activity was attributed to a sensitization mechanism, involving surface NH_x species. Similar sensitization reactions have been described, for instance, during NO reduction with participation of NH_2 donor levels in adsorbed NH_3 on TiO_2 [18]. The direct electron transfer from the adsorbed molecule to the conduction/valence band of the semiconductor results in a red shift of the effective wavelength of the photocatalyst.

This work further investigated the influence of N species in the photocatalytic properties of N—TiO_2 thin films deposited using different N precursors, namely *tert*-butylamine, benzylamine and ammonia. The use of these precursors was intended to create different synthesis environments. As a rule of thumb, oxygen-rich conditions, such as those used in wet processes (sol-gel, etc.) induced the formation of interstitial N(i) and NO_x species, whilst oxygen-deficient (reducing) conditions would favor the incorporation of N(s) in O lattice sites. An empirical approach is used to establish correlation between parameters such as crystallinity, film thickness, nitrogen chemical state and nitrogen concentrations with the photocatalytic behavior of N—TiO_2 films under UV and visible light illumination.

2. Materials and methods

2.1. Chemical vapor deposition apparatus and film synthesis

All chemicals were purchased from *Sigma-Aldrich* unless stated otherwise. The deposition of TiO_2 films was carried out using titanium tetrachloride ($TiCl_4$, 99.9%) and ethyl acetate ($C_4H_8O_2$, 99%) as titanium and oxygen sources, respectively. In the case of nitrogen-doped films, *tert*-butylamine ($C_4H_{11}N$ 99.5%), benzylamine (C_7H_9N 99%) or ammonia (NH_3, oxygen free, from *BOC*) were used as the nitrogen source. All precursors were contained in stainless steel bubblers at appropriate temperatures in order to generate sufficient vapor pressure to be carried through the CVD rig. All components of the CVD apparatus were at high temperature (150 °C). The gases were mixed in stainless steel mixing chambers at 250 °C and carried into the CVD reactor through a double baffle manifold using pre-heated N_2 gas (from *BOC*). The CVD reactor consisted of a 320 mm-long graphite block with three inserted *Whatman* heater cartridges. Pt-Rh thermocouples were used to control the temperature of the individual components of the rig.

In a typical deposition, the bubbler temperatures of titanium, oxygen and nitrogen precursors were set at 68, 38 and 5 °C, respectively. The latter temperature was achieved using an ice bath and it applies to both *tert*-butylamine and benzylamine; ammonia flowed under its own vapor pressure from a gas cylinder. The corresponding mass flow rates of titanium and oxygen sources were 6.7×10^{-3} and 3.1×10^{-3} g min^{-1}. The mass flow rate conditions of the N precursors are indicated in Table 1. The films were deposited at 500 °C on float glass substrates ($90 \times 225 \times 4$ mm^3, *Pilkington NSG Group*). The glass substrates included a silica (SiO_2) barrier layer to prevent ion diffusion into the deposited film. The substrates were thoroughly cleaned using acetone (C_3H_6O 99%), isopropanol (C_3H_8O 99.9%) and distilled water and dried in air prior to use. Once coated, the large substrates were cut into small samples (25×25 mm^2) and selected from different regions

Table 1
Synthesis conditions and properties of N—TiO_2 films. Titanium tetrachloride, $TiCl_4$ (6.7×10^{-3} g min^{-1}), ethyl acetate, $C_4H_8O_2$ (3.1×10^{-3} g min^{-1}) were used as titanium and oxygen precursors, respectively. Tert-butylamine (TBA), benzylamine (BA) or ammonia were used as nitrogen precursors as indicated. The corresponding deposition times (t) were as indicated. The corresponding photocatalytic activities are given as formal quantum efficiency (ξ, units: molec photon^{-1}) and expressed as stearic acid molecules degraded per incident photon. The N concentrations in the films were estimated from XPS data (error, ±10 at%).

Sample #	N Precursor	N Mass Flow/10^{-4} (g min^{-1})	Bulk N species (at%)		Surface N(i) (at%)	t (s)	Film thickness (nm)	ξ/10^{-4} (molec photon^{-1})
			N(i)	N(s)				
Ti1	–	–	–	–	–	60	253 ± 35	0.63
Ti2	–	–	–	–	–	120	744 ± 72	0.92
NTi1	NH3	4040	1.69	7.75	3.70	60	370 ± 80	0.10
NTi2	TBA	59.40	0.94	4.43	2.08	60	290 ± 25	0.35
NTi3	TBA	12.70	0.37	1.51	4.13	60	237 ± 63	1.06
NTi4	BA	0.03	0.41	0.27	3.04	60	461 ± 57	1.01
NTi5	TBA	13.50	0.23	0.65	3.06	60	334 ± 45	1.23
NTi6	NH3	760	0.21	0.41	3.79	60	370 ± 36	0.04
NTi7	BA	0.08	0.15	0.18	1.82	60	555 ± 35	0.07
NTi8	BA	0.02	0.11	0.13	3.19	60	468 ± 40	2.30
NTi9	BA	0.11	0.10	0.14	2.46	60	584 ± 49	0.05
NTi10	BA	0.02	0.08	0.13	1.80	60	357 ± 20	0.07
NTi11	BA	0.02	0.01	0.11	0.64	60	416 ± 40	1.24
NTi12	BA	0.02	0.08	0.15	0.66	60	483 ± 67	1.11
NTi13	TBA	13.50	0.11	0.26	1.56	120	665 ± 32	2.57
NTi14	TBA	13.50	0.06	0.14	0.93	120	703 ± 60	1.30

of the CVD reactor. The nitrogen precursors were introduced into the reactor in a *combinatorial* fashion through a different mixing chamber. This means that the resulting film contained a gradient of N concentrations across the large substrates. These concentrations were intrinsically linked not only to the experimental conditions (flow rates and temperatures) but also to their relative position in the reactor. The experiments described here were carried out using selected samples (named here as NTi1-NTi14) which contained constant nitrogen concentrations.

2.2. Analytical methods

X-ray diffraction (XRD) studies were performed using a Bruker-Axs D8 (GADDS) diffractometer, equipped with a monochromated Cu X-ray source ($K\alpha_1$, 1.5406 Å) and a 1D area X-ray detector with a resolution of 0.01°. The films were analyzed with a glancing incident angle (θ) of 1°. The diffraction patterns obtained were compared with database standards from International Centre for Diffraction Data (ICDD). Raman spectroscopy was carried out using a Renishaw 1000 spectrometer equipped with a 514-nm laser. The Raman system was calibrated using a silicon reference. Absorption spectroscopy was performed using a double beam, double monochromated Perkin Elmer Lambda 950 UV/Vis/NIR Spectrophotometer. Reflectance spectra was recorded for different positions in the range 300–2500 nm on a Helios double beam instrument standardized relative to a silicon mirror, which allowed to determine the thickness of the films *via Swanepoel* method [19]. These measurements were confirmed using side-view scanning electron microscopy (SEM). SEM analysis was carried out using secondary electron image on a JEOL 6301 field-emission instrument (5 kV). X-Ray photoelectron spectroscopy (XPS) was performed using a Thermo K-alpha spectrometer with monochromated Al K alpha radiation, a dual beam charge compensation system and constant pass energy of 50 eV. Survey scans were collected in the energy range of 0–1200 eV. High-resolution peaks were used for the principal peaks Ti(2p), O(1s), N(1s), C(1s) and Si(2p). The peaks were modelled using sensitivity factors to calculate the film composition. The area underneath these bands is an indication of the concentration of element within the region of analysis (spot size 400 μm).

2.3. Photocatalytic tests

The photocatalytic activity of the films was evaluated during degradation of octadecanoic (stearic) acid, a model organic pollutant [20,21]. A thin layer of stearic acid was deposited by dip-coating into a 0.05 M of the acid in chloroform solution. A *Perkin Elmer RX-I* infrared spectrometer was used to monitor the acid C—H bands in the range of 2700–3000 cm^{-1}. The photocatalytic rates were estimated from linear regression of the corresponding degradation curves (integrated areas *vs* irradiation time), using the conversion factor 1 $cm^{-1} \equiv 9.7 \times 10^{+15}$ molecules from the literature [20]. The as-deposited films were treated under UVA light in humid air conditions over 24 h and kept in the dark for at least 24 h previous to any photocatalytic experiment. The photocatalytic tests were carried out under UVA ($\lambda = 365$ nm) or visible light irradiation. Blacklight-bulb lamps (*Vilber-Lourmat*, 2×8 W, 1.2 mW cm^{-2}) were used in the UV tests and their irradiance was measured using a UVX meter (*UVP*). The visible light tests were carried out using a 75 W Xe lamp with AM 1.5G and cut-off filters ($\lambda > 420$ nm). A commercial (*Evonik*) P25 TiO_2 film was used as a standard reference in order to test any potential UV component leaking through the filter. The film was dip-coated onto a glass substrate from a 5 wt% TiO_2 dispersion and pre-irradiated (UVC treatment) before use.

3. Results and discussion

The TiO_2 thin films were deposited from titanium chloride ($TiCl_4$) and ethyl acetate ($C_4H_8O_2$) on float glass at 500 °C using APCVD as described in the experimental section. A nitrogen source, either *tert*-butylamine ($C_4H_{11}N$), ammonia (NH_3) or benzylamine (C_7H_9N), was incorporated in the case of the N—TiO_2 films. These samples will be henceforth referred to as Ti and NTi for undoped and N–doped TiO_2 films, respectively (Table 1). Under typical synthesis conditions, the decomposition of *tert*-butylamine is expected to occur readily by a dual molecular-split type mechanism resulting in the formation of C_3NH_7, NH_3 and CH_4, among other products [22]. On the other hand, ammonia has a very low decomposition rate and benzylamine will largely remain unchanged [23,24]. However, their respective decomposition rates would be influenced by contact with the substrate surface.

The incorporation of nitrogen was first evidenced by a color change of the as-deposited films. The undoped TiO_2 films were colorless with an absorption onset at λ∼380 nm (Fig. 1a). In contrast, the N—TiO_2 films were yellow and their corresponding optical spectra was red-shifted with respect to that of the pure TiO_2 films. This redshift has been widely observed in the literature [1,2,12,25–27], however no correlation with nitrogen content has been established. This is not surprising since many N species have been assigned to similar binding energies around 400 eV and establishing the impact of these species over the optical properties of the films would be arduous. This is clearly shown in Fig. 1b,

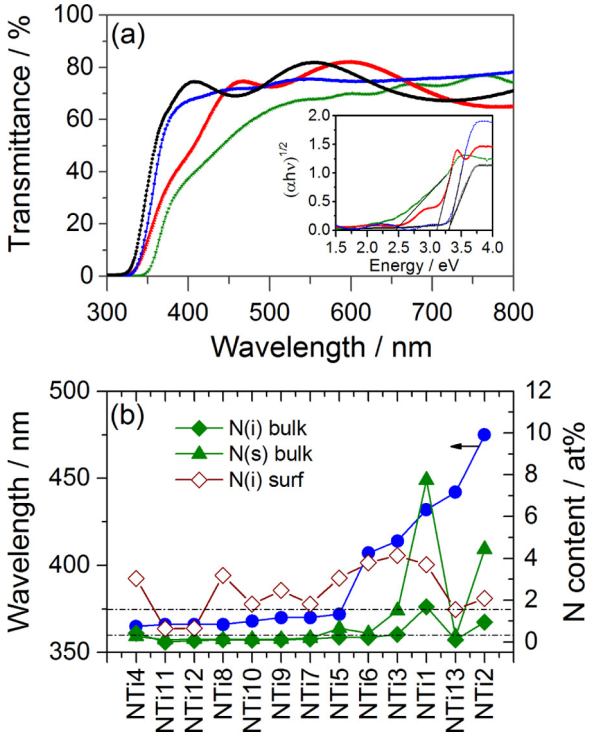

Fig. 1. UV/Vis spectra of pristine (black line) and selected N—TiO_2 films: Ti1 (black line), NTi8 (blue line), NTi6 (red line) and NTi13 (green line) deposited using benzylamine, ammonia or *tert*-butylamine as the nitrogen precursor, respectively. Inset: Tauc plots assuming all films are indirect bandgap semiconductors. (b) Shift in optical transmission at 50% (full blue circles) and corresponding nitrogen content in the films, given as interstitial (N(i), full green diamonds) and substitutional (N(s), full green triangles) nitrogen species in the bulk, as well as N(i) groups (empty red diamonds) at the surface. The samples are arranged on the basis of increasing optical shift for clarity. The dashed horizontal lines indicate the optical shift (50%) for a range of undoped TiO_2 films of corresponding thicknesses (For interpretation of the references to colour in this figure legend, the reader is referred to the web version of this article.).

which compares the trend of the shift at 50% transmission with the nitrogen content in the films, as detected by XPS studies (Table 1). A close inspection of Fig. 1b shows, for instance, a substantial shift for sample NTi6, despite the relatively low nitrogen levels detected in this film. It is tempting to establish correlation between the optical features of N—TiO_2 materials and potential changes in bandgap energy (E_{bg}). This is typically carried out by Tauc analysis (Fig. 1a, inset) from the corresponding Kubelka-Munk functions, assuming that the doped films are indirect bandgap semiconductors like pristine TiO_2. It is however important to take into account that the redshift observed could also be due to changes in the morphology and microstructure of the films, since they were deposited under different chemical environments [28]. In the case of the pristine TiO_2 films, a small shift of up to 15 nm was observed in the range of thicknesses studied here (dashed horizontal lines in Fig. 1b). This redshift was likely due to changes in particle size and film thickness. The typical surface morphologies of the films deposited at t = 60 and 120 s are shown in Fig. 2. In the case of the undoped films, sample Ti1 (t = 60 s) showed small round particles with average size of ~20 nm (Fig. 2a) whilst sample Ti2 (t = 120 s) contained large star-like aggregated particles with average size of ~200 nm (Fig. 2c). In general, the incorporation of low concentrations of nitrogen did not affect the surface morphology of the TiO_2 films (Fig. 2d). However, substantial surface deterioration was apparent when using ammonia (Fig. 2b), likely due to the reducing environment during the deposition of the films. This is in agreement with literature reports [12,29,30] and it was certainly observed in the case of sample NTi6, for instance.

Further structural analysis was carried out using X-ray diffraction and Raman spectroscopy. Raman analysis confirmed the presence of anatase TiO_2 and no additional phases were detected in the films. The main diffraction peak (101) of the anatase phase at 25.4° (2θ) is shown in Fig. 3a for selected films (the inset figure shows the full pattern of a highly crystalline N—TiO_2 film). The incorporation of relatively high concentrations of nitrogen (>1 at%) is known to affect the crystallinity of N—TiO_2 materials [12,29–31], which may come at the expense of photocatalytic activity. This was the case of samples NTi1 and NTi2, for instance, which showed very poor crystallinity and the anatase phase was hardly recognizable from the XRD data. In order to minimize this effect, the N levels were controlled below 1 at%. The (101) peak shifted upon relatively high concentrations of nitrogen, as a result of changes in unit cell parameters (Fig. 3b). However, most undoped and doped films showed similar peak features. It is worth noting that, despite the similarities, the photocatalytic activities of N—TiO_2 films did not follow a linear trend with crystallinity, as expected from pristine TiO_2 samples within the range of thicknesses studied here (Fig. 3c). Instead, many N—TiO_2 films showed significantly enhanced activities under UVA illumination.

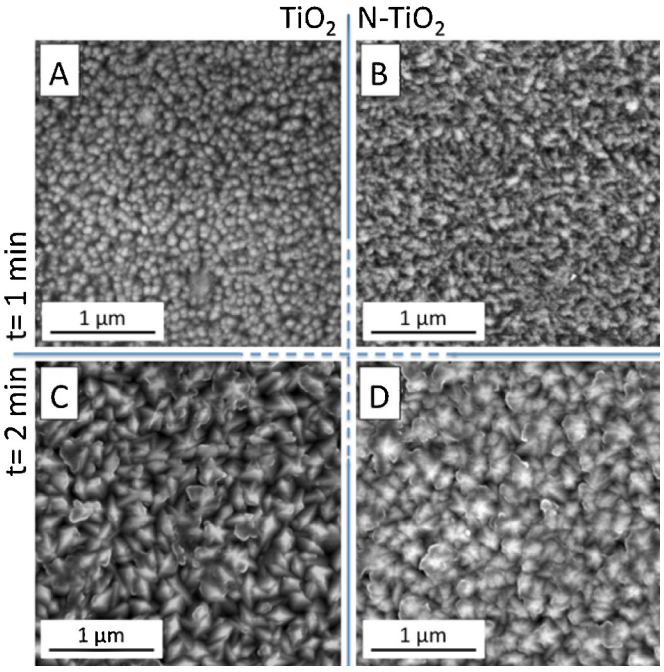

Fig. 2. Scanning electron microscopy (SEM) images of TiO_2 (left column, A,C) and N–TiO_2 (right column, B,D) films. Top row: films deposited for t = 1 min; bottom row: films deposited for t = 2 min. The specific samples are: (A) Ti1; (B) NTi6 (C) Ti2; (D) NTi8, as described in Table 1.

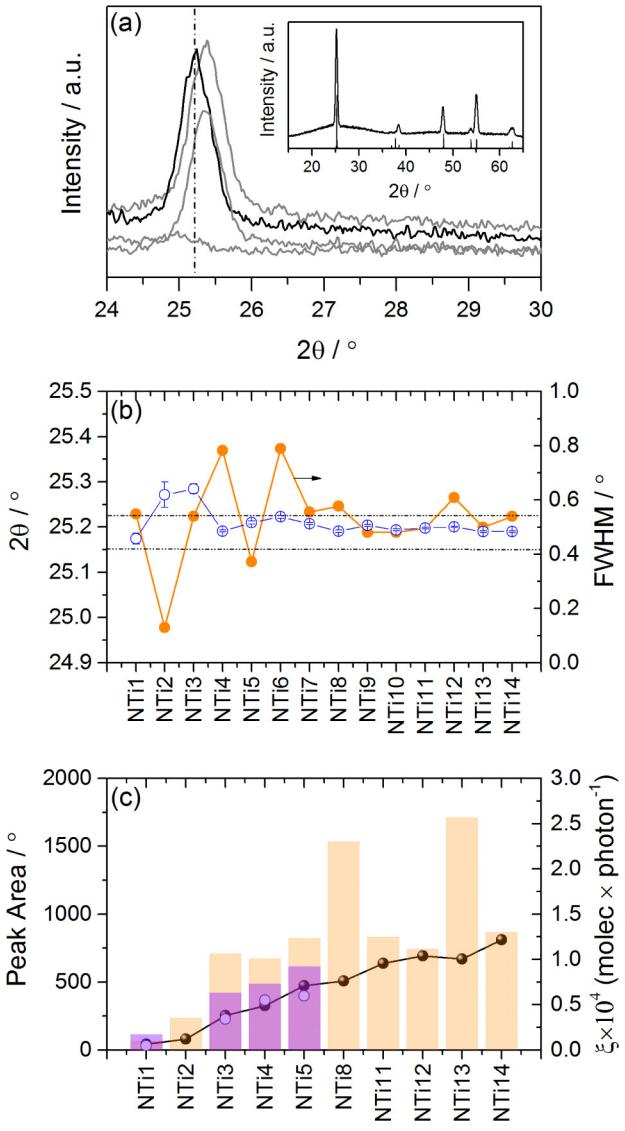

Fig. 3. (a) (101) diffraction peak of the anatase structure in undoped TiO_2 (black line) and selected N—TiO_2 films. Inset: typical XRD pattern of a highly crystalline N—TiO_2 film (λ=1.5406 Å). The vertical lines in the inset figure correspond to theoretical diffraction peaks of the anatase phase. (b) Corresponding peak centers (full orange symbols) and full width at half maxima (empty blue symbols) of the (101) peak from XRD data. The dashed horizontal lines indicate the region expected for undoped TiO_2 samples of different physical characteristics (crystallinity, thickness, etc.). (c) Peak areas of the (101) peak of TiO_2 (empty symbols) and N—TiO_2 (full symbols) anatase structures and corresponding photocatalytic activities, given as formal quantum efficiency (ξ, units: molec photon^{-1}), illustrated as purple (TiO_2) and beige (N—TiO_2) bars (For interpretation of the references to colour in this figure legend, the reader is referred to the web version of this article.).

Inspection of the *N 1s* environment revealed the presence of both N(s) (396–397 eV) and N(i) (~400 eV) species during XPS depth profile analysis (Table 1). This could be due to oxidation/reduction processes of the bulk N groups during the ion etching. However, we tested a range of N-containing samples (nitrides, amines, etc.) and the only changes observed indicated an increasing formation of nitrite (NO_2) and nitrate (NO_3) groups and thus, oxidation of the N groups. Hence, it was confidently assumed that the N(s), formally N^{3-} species in the bulk, were introduced during the deposition of the films. Surface analysis of the films showed N(i) groups with binding energies at ~400 eV, independently of the nitrogen precursor used. Very weak features (shoulders) were also identified at 398.5–399 eV, which have been assigned to substitutional N—O and O—N—O species [8]. In the case of *tert*-butylamine, these were the only species detected on the surface of the films (Fig. 4a) whilst the use of benzylamine often introduced additional groups with binding energies at 401–402 eV (Fig. 4b). The latter has been assigned to adsorbed N—O groups (N—O—Ti—O or O—N—Ti—O) [32,33]. On the other hand,

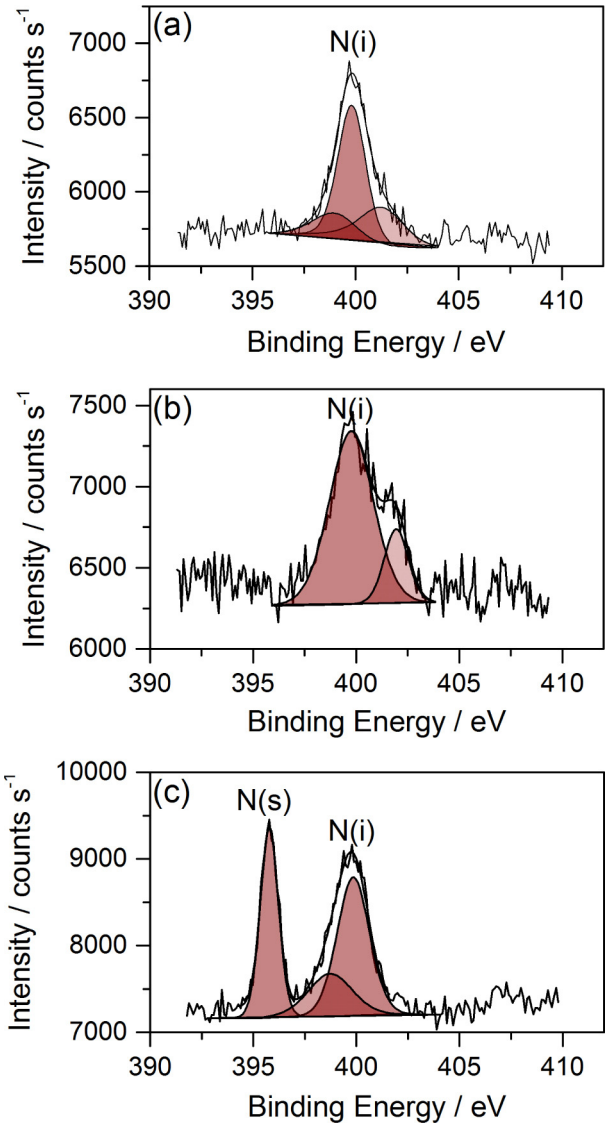

Fig. 4. Surface X-ray photoelectron spectra (XPS) in the *N* 1s environment of N—TiO_2 films as deposited using (a) *tert*-butylamine (NTi13), (b) benzylamine (NTi9) or (c) ammonia (NTi1) as nitrogen precursor. N(s) and N(i) correspond to N^{3-} (substitutional) and N^0 (interstitial) species, respectively.

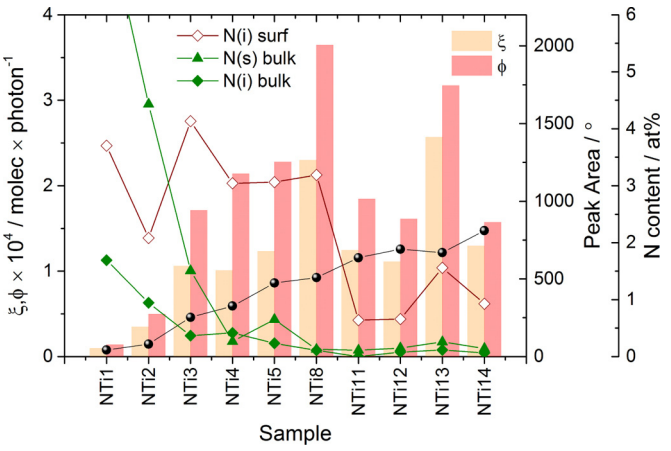

Fig. 5. Photocatalytic activities of N—TiO_2 films under UVA light, given as formal quantum efficiencies (ξ) and quantum yields (ϕ;), and corresponding nitrogen levels given as bulk substitutional (full triangles), bulk interstitial (full diamonds) and surface interstitial (empty diamonds) species. Peak areas of the (101) peak of the anatase structure (full black symbols) are given for reference.

the reducing conditions when using ammonia favored the introduction of N(s) species, as evidenced for sample NTi1 (Fig. 4c).

In Fig. 5, the photocatalytic activities of N—TiO_2 films are compared with levels of bulk N(s) and N(i) as well as surface N(i) species. In this case, the activities are given as formal quantum efficiencies, ξ (units: molecules photon^{-1}) –defined as molecules degraded per *incident* photon, and quantum yields, ϕ; (units: molecules photon^{-1}), which accounts for molecules degraded per *absorbed* photon. Considering the issues raised in the discussion of the optical properties of the films, the ϕ; values should only be considered as for comparison purposes. These values were roughly estimated from the fraction of light absorbed by the films at 365 nm. It is worth noting that both ξ and ϕ; values followed a similar trend. It was first evident (Fig. 5) that the trend of activities did not follow the bulk N content in the films. It may also be inferred that relatively high bulk N(s) concentrations compromised the crystallinity of samples [31], which likely affected the photocatalytic efficiencies of all samples up to NTi5. Close inspection of the highly crystalline samples (NT11–NT14 group) shows similar activities except that for NTi13, which was significantly high. In this case, the photocatalytic activities followed the trend of surface N(i) species with binding energies at ~400 eV, in agreement with our previous results [17]. On the other hand, samples NTi5 and NTi8 had similar surface N(i) content and comparable crystallinity, however the photocatalytic activity of sample NTi8 was remarkably higher than that of NTi5. This was attributed to a potential impact of bulk N(s) species in the latter case. These species can act as charge recombination centers, affecting the photocatalytic activity of N-doped materials under UVA irradiation [34]. Further evidence of the impact of bulk N(s) species may be responsible for the unexpectedly low activity of sample NTi3 compared to that of NTi4. Both samples showed similar diffraction features but different surface N(i) content, favoring sample NTi3. Nonetheless, the latter also contained high bulk N(s) levels, which allegedly affected its photocatalytic efficiency.

It is important to note that we excluded from this empirical analysis all the samples containing *additional* surface N species other than those with binding energies at ~400 eV. In our previous work [17], the presence of amine groups (NH_x) with binding energies at ~400 eV was suggested to photosensitize the degradation of stearic acid under UVA illumination. It was observed that the apparent or *extrinsic* photocatalytic activity decreased drastically once these species were consumed in the

reaction. The presence of additional surface species was found highly detrimental to the photocatalytic performance of N—TiO_2 films. Accordingly, some films such as NTi7, NTi9 and NTi10, which had otherwise similar structural features and bulk N levels than those of samples NTi8 or NTi11, were unexpectedly inactive (Table 1). The impact of nitrogen species is summarized in Fig. 6. Only N—TiO_2 films containing N surface species with binding energy at ~400 eV alone were highly active compared to similar undoped films under UVA illumination and their activity correlated with the concentration of these surface species. However, films showing N—O groups at 401 – 402, ~403 (NO_2) or 408 (NO_3) eV were inactive.

Further photocatalytic testing of the N—TiO_2 films was carried out under visible light using a 75 W Xe lamp (AM 1.5 G, λ > 420 nm) over 70 h. The *apparent* rates of degradation of stearic acid molecules (R_{SA}, units: molec cm^{-2} s^{-1}) on selected N—TiO_2 films are shown in Fig. 7(a). Similar plots are often reported in the literature and it was tempting to correlate these activities with the N content in the films. Nonetheless, the validity of the test was compromised by the apparent activity of the undoped film (Ti2), which points to potential UV leaking through the cut-off filter, as well as the poor fitting of the degradation curves ($r^2 < 0.90$), indicating that no visible light activity could be determined beyond instrumental error. Indeed, as shown in Fig. 7(b), the apparent activity of NTi3 was negligible compared with that of a standard *Evonik* P25 dip-coated film [35] under identical conditions. Thus, a potential visible light sensitization mechanism with participation of NH_x groups, as described by *Tanaka* et al. [18], could not be confirmed.

It is important to note that our observations regarding the impact of surface N—O species during photocatalytic experiments are in contrast to those reported by some authors. For instance, *Kisch* et al. [36] reported visible light activity of N–TiO_2 materials containing surface N(i) groups at binding energies of ~400 eV, during mineralization of various model organic pollutants. These authors have also reported on a visible light active N–TiO_2 material containing a single surface peak at 404 eV, which was assigned as hyponitrite groups (NO^-) [37]. However, these materials were synthesized from titanium hydroxide and urea and their studies revealed the presence of surface carbonaceous species. It is not clear whether such species could have a role in a potential sensitization process to encourage visible light absorption in these compounds [20,38].

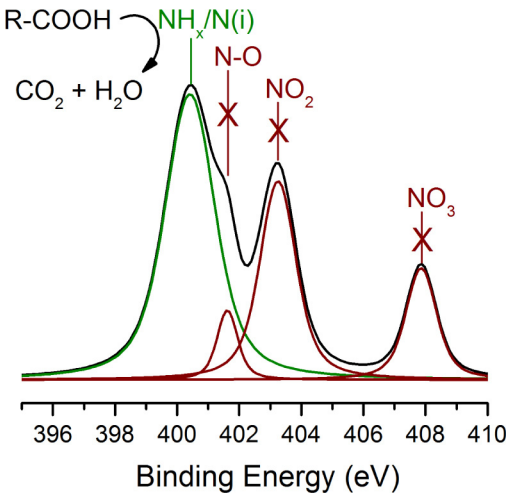

Fig. 6. Schematic figure summarizing the influence of surface N species on the photocatalytic activity of N—TiO_2 films under UVA illumination, as observed here and in our previous work [17]. Films containing adsorbed N species at ~400 eV (N(i) or NH_x) showed an apparent enhancement in activity (*sensitized* films). However, the presence of N—O groups at binding energies of 401–402, 403 and 408 eV were highly detrimental to their efficiency under UV illumination.

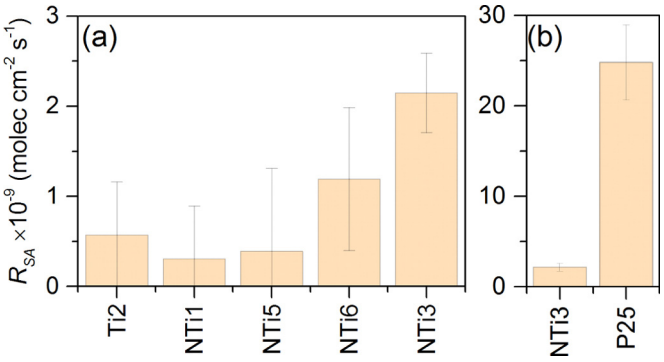

Fig. 7. (a) *Apparent* visible light activity, given as rate of degradation of stearic acid (R_{SA}), of selected N—TiO_2 films and (b) comparison between the corresponding activities of the best N—TiO_2 sample (NTi3) and a dip-coated P25 TiO_2 film.

4. Conclusions

A range of N–TiO_2 thin films were deposited on glass by atmospheric-pressure CVD from titanium chloride, ethyl acetate and different N precursors, namely ammonia, benzylamine and *tert*-butylamine. Both interstitial and substitutional N species were identified in the films independently of the precursor used. The use of *tert*-butylamine was found convenient for the control of N levels in the films and it often resulted in species with binding energies at ~400 eV, which favored the apparent photocatalytic activity of the films in the UV range. This is in agreement with previous results and the enhanced activity observed was attributed to a *sensitization* mechanism. As an alternative N precursor, benzylamine often resulted in additional surface species (N—O—Ti—O or O—N—Ti—O) at 401–402 eV that deactivated the films. On the other hand, the reducing conditions when using ammonia favored the incorporation of substitutional N groups (in oxygen sites), which were identified at binding energies of ~396 eV. Unfortunately, in our case, the chemical environment under ammonia affected the crystallinity and surface integrity of the films.

Following an empirical approach based on their structural properties, as studied by X-ray diffraction, it was possible to establish correlation between the photocatalytic activities observed under UV irradiation and the nitrogen content in the N—TiO_2 films. In particular, the activities of highly crystalline samples and negligible bulk nitrogen content clearly followed the trend of surface nitrogen groups, N(i), at ~400 eV, which confirmed our previous results. It was difficult to establish this correlation among poorly crystalline samples, but we also pointed out that the presence of relatively high levels of bulk N groups may be detrimental for the activity of the films, as they may act as recombination centers.

Despite the different synthesis conditions used, no visible light activity was observed beyond instrumental error. The implementation of visible light activity of N—TiO_2 compounds will involve a number of crucial elements, including a selective type of surface species and a restricted number of lattice defects for the promotion of charge diffusion. From these results, it was not clear whether the visible light activity would come from the effect of an optimum concentration of N(s) species (396–397 eV), as long as these do not compromise the structural properties of the film. Certainly, the potential presence of these species in the bulk of the N—TiO_2 films, as analyzed by XPS, did not encourage visible light activity in this work. It is also unclear whether the presence of certain N(i) species

at 400 eV may be detrimental for their photocatalytic performance in the visible range.

Acknowledgements

This work was supported by the Engineering and Physical Sciences Research Council (EPSRC, Grant N. EP/L017709). RQC and CVS would like to thank the European Union's Seventh Framework Programme (FP7, PCATDES project, grant N. 309846) for their support. Drs. Robert Palgrave, Christopher Blackman, Michael Powell and Emily Glover are thanked for discussion on XPS analysis. Dr. Steve Firth and Martin Vickers are thanked for access to SEM and XRD instruments.

References

[1] R. Asahi, T. Morikawa, H. Irie, T. Ohwaki, Nitrogen-doped titanium dioxide as visible-light-sensitive photocatalyst: designs, developments, and prospects, Chem. Rev. 114 (2014) 9824–9852.
[2] A.V. Emeline, V.N. Kuznetsov, V.K. Rybchuk, N. Serpone, Visible-light-active titania photocatalysts: the case of N-doped TiO_2?properties and some fundamental issues, Int. J. Photoenergy 2008 (2008) 258394–258413.
[3] T.L. Thompson, J.T. Yates, Surface science studies of the photoactivation of TiO_2–new photochemical processes, Chem. Rev 106 (2006) 4428–4453.
[4] M. Pelaez, N.T. Nolan, S.C. Pillai, M.K. Seery, P. Falaras, A.G. Kontos, P.S.M. Dunlop, J.W.J. Hamilton, J.A. Byrne, K. O'shea, M.H. Entezari, D.D. Dionysiou, A review on the visible light active titanium dioxide photocatalysts for environmental applications, Appl. Catal. B Environ. 125 (2012) 331–349.
[5] Y. Taga, Titanium oxide based visible light photocatalysts: materials design and applications, Thin Solid Films 517 (2009) 3167–3172.
[6] Y. Paz, Application of TiO_2 photocatalysis for air treatment: patents' overview, Appl. Catal. B Environ. 99 (2010) 448–460.
[7] B. Viswanathan, K.R. Krishanmurthy, Nitrogen incorporation in TiO_2: does it make a visible light photo-active material? Int. J. Photoenergy 2012 (2012) 269654-1/–10..
[8] R. Asahi, T. Morikawa, Nitrogen complex species and its chemical nature in TiO_2 for visible-light sensitized photocatalysis, Chem. Phys. 339 (2007) 57–63.
[9] N.C. Saha, H.G. Tompkins, Titanium nitride oxidation chemistry: an X-ray photoelectron spectroscopy study, J. Appl. Phys. 72 (1992) 3072–3079.
[10] C. Di Valentin, G. Pacchioni, A. Selloni, S. Livraghi, E. Giamello, Characterization of paramagnetic species in N-doped TiO_2 powders by EPR spectroscopy and DFT calculations, J. Phys. Chem. B 109 (2005) 11414–11419.
[11] O. Diwald, T.L. Thompson, T. Zubkov, E.G. Goralski, S.D. Walck, J.T. Yates, The effect of nitrogen ion implantation on the photoactivity of TiO_2 rutile single crystals, J. Phys. Chem. B 108 (2004) 6004–6008.
[12] M. Batzill, E.H. Morales, U. Diebold, Influence of nitrogen doping on the defect formation and surface properties of TiO_2 rutile and Anatase, Phys. Rev. Lett. 96 (2006) 026103-1/–4.
[13] W. Balcerski, S.Y. Ryu, M.R. Hoffmann, Visible-light photoactivity of nitrogen-doped TiO_2: photo-oxidation of HCO_2H to CO_2 and H_2O, J. Phys. Chem. C 111 (2007) 15357–15362.
[14] Z. Lin, A. Orlov, R.M. Lambert, M.C. Payne, New insights into the origin of visible light photocatalytic activity of nitrogen-doped and oxygen-deficient anatase TiO_2, J. Phys. Chem. B 109 (2005) 20948–20952.
[15] G. Barolo, S. Livraghi, M. Chiesa, M.C. Paganini, E. Giamello, Mechanism of the photoactivity under visible light of N-doped titanium dioxide. Charge carriers migration in irradiated N-TiO_2 investigated by electron paramagnetic resonance, J. Phys. Chem. C 116 (2012) 20887–20894.
[16] Y. Nosaka, M. Matsushita, J. Nishino, A.Y. Nosaka, Nitrogen-doped titanium dioxide photocatalysts for visible response prepared by using organic compounds, Sci. Technol. Adv. Mat. 6 (2005) 143–148.
[17] R. Quesada-Cabrera, C. Sotelo-Vazquez, J.A. Darr, I.P. Parkin, Critical influence of surface nitrogen species on the activity of N-doped TiO_2 thin-films during photodegradation of stearic acid under UV light irradiation, Appl. Catal. B Environ. 160-161 (2014) 582–588.
[18] T. Shishido, K. Teramura, T. Tanaka, Photo-induced electron transfer between a reactant molecule and semiconductor photocatalyst: in situ doping, Catal. Surv. Asia 15 (2011) 240–258.
[19] R. Swanepoel, Determination of the thickness and optical constants of amorphous silicon, J Phys. E: Sci. Instrum. 16 (1983) 1214–1222.
[20] A. Mills, J.S. Wang, Simultaneous monitoring of the destruction of stearic acid and generation of carbon dioxide by self-cleaning semiconductor photocatalytic films, J. Photochem. Photobiol. A Chem. 182 (2006) 181–186.
[21] R. Quesada-Cabrera, A. Mills, C. O'Rourke, Action spectra of P25 TiO_2 and a visible light absorbing carbon-modified titania in the photocatalytic degradation of stearic acid, Appl. Catal. B Environ. 150 (2014) 338–344.
[22] H.O. Pritchard, R.G. Sowden, A.F. Trotman-Dickenson, The thermal decomposition of tert-butylamine, J.Chem.Soc 54 (1954) 546–549.
[23] C.D. Hurd, F.L. Carnahan, The action of heat on ethylamine and benzylamine, J. Am. Chem. Soc. 52 (1930) 4151–4158.
[24] A.H. White, Wm. Melville, Decomposition of ammonia at high temperatures, J. Am. Chem. Soc 27 (1905) 373–386.
[25] V.N. Kuznetsov, N. Serpone, On the origin of the spectral bands in the visible absorption spectra of visible-light-active TiO_2 specimens analysis and assignments, J. Phys. Chem. C 113 (2009) 15110–15123.
[26] T. Morikawa, R. Asahi, T. Ohwaki, K. Aoki, Y. Taga, Band-gap narrowing of titanium dioxide, Japan. J. Appl. Phys. 40 (2001) L561–L563.
[27] P.-G. Wu, C.-H. Ma, J.K. Shang, Effects of nitrogen doping on optical properties of TiO_2 thin films, Appl. Phys. A 81 (2005) 1411–1417.
[28] A.B. Murphy, Band-gap determination from diffuse reflectance measurements of semiconductor films, and application to photoelectrochemical water-splitting, Sol, Energ. Mat. Sol. C. 91 (2007) 1326–1337.
[29] U. Diebold, The surface science of titanium dioxide, Surf. Sci. Rep. 48 (2003) 53–229.
[30] H.M. Yates, M.G. Nolan, D.W. Sheel, M.E. Pemble, The role of nitrogen doping on the development of visible light-induced photocatalytic activity in thin TiO_2 films grown on glass by chemical vapour deposition, J. Photochem. Photobiol. A Chem. 179 (2006) 213–223.
[31] C. Sotelo-Vazquez, R. Quesada-Cabrera, J.A. Darr, I.P. Parkin, Single-step synthesis of doped TiO2 stratified thin-films by atmospheric-pressure chemical vapour deposition, J. Mater. Chem. A 2 (2014) 7082–7087.
[32] C.S. Gopinath, Comment on Photoelectron Spectroscopic Investigation of nitrogen-doped titania nanoparticles, J. Phys. Chem. B 110 (2006) 7079–7080.
[33] J.A. Rodriguez, T. Jirsak, G. Liu, J. Hrbek, J. Dvorak, A. Maiti, Chemistry of NO_2 on oxide surfaces: formation of NO_3 on TiO_2(110) and NO_2(O vacancy interactions, J. Am. Chem. Soc. 123 (2001) 9597–9605.
[34] S.-Z. Chen, P.-Y. Zhang, D.-M. Zhuang, W.-P. Zhu, Catal. Commun. 5 (2004) 677–680.
[35] A. Mills, J.S. Wang, Photomineralisation of 4-chlorophenol sensitised by TiO_2 thin films, J. Photochem. Photobiol. A Chem. 118 (1998) 53–63.
[36] H. Kisch, S. Sakthivel, M. Janczarek, D. Mitoraj, A low-band gap, nitrogen-modified titania visible-light photocatalyst, J. Phys. Chem. C 111 (2007) 11445–11449.
[37] S. Sakthivel, H. Kisch, Photocatalytic and photoelectrochemical properties of nitrogen-doped titanium dioxide, ChemPhysChem 4 (2003) 487–490.
[38] P. Zabek, J. Eberl, H. Kisch, On the origin of visible light activity in carbon-modified titania, Photochem. Photobiol. Sci. 8 (2009) 264–269.